Iterative Equalization for SOQPSK in Multipath Fading

Qiang Lei and Michael Rice

Telemetry Laboratory
424 Clyde Building
Brigham Young University
Provo, UT 84602

ABSTRACT

This paper investigates the application of iterative equalization techniques to overcome multipath fading for shaped offset QPSK (SOQPSK) in aeronautical telemetry. Two iterative equalization techniques for turbo encoded SOQPSK are presented. The first is the optimal-MAP turbo equalizer for OQPSK. The second equalizer is the adpative decision feedback equalizer. Simulation shows that in the presence of frequency selective multipath typically encountered in aeronautical telemetry, both of these equalizers exhibit impressive performance.

KEY WORDS

Multipath Fading, Iterative Equalization, SOQPSK

INTRODUCTION

The data rates required in aeronautical telemetry have increased dramatically from 100 kbits/sec in the early 1970s to 10-20 Mbits/sec today. The consequence of this trend is the multipath interference encountered in aeronautical telemetry has become frequency selective. The data links used in aeronautical telemetry are subject to multipath interference in the form of strong “ground bounces” (especially at low elevation angles) and reflections off irregular terrain [1][2]. At low data rates, such as 100 kbits/sec, the multipath interference appears as flat fading across the signal bandwidth. At high data rates, the signal bandwidth is much wider and the multipath interference is characterized by deep spectral nulls. The frequency selective nature of the multipath interference disrupts the data link and is the main cause of data loss in aeronautical telemetry.

Equalization is a well-known multipath mitigation technique [3]. Motivated by the impressive gains of turbo coding, turbo equalization has also been investigated. The concept of turbo equalization was first proposed by Douillard et. al. [4], and further developed in [5, 6, 7, 8] where it was shown that turbo equalization yields greater improvement than separate equalization and decoding. The optimal iterative equalizer is based on a maximum *a posteriori* (MAP) estimate of the channel state and is aided by iterating with a soft-output decoder (e.g., SOVA with convolutional codes or MAP with turbo codes). The complexity of the channel iterative MAP equalizer can be prohibitive in some applications. Consequently, suboptimum approaches such as linear equalizers and decision feedback equalizers have been incorporated into an iterative processing structure [6, 7, 8]. Douillard's work on turbo equalization focused on a turbo-equalizer/convolutional-code combination [4]. Subsequent work (cf., [5]) explored the performance of a turbo-equalizer/turbo-code combination. This latter combination outperforms the former combination.

This paper explores the application of iterative equalization technique to shaped offset QPSK (SOQPSK) which is defined in aeronautical telemetry standard IRIG-106 [9]. We demonstrate that the MAP equalizer designed for unshaped OQPSK, is also capable of achieving impressive gains for SOQPSK in the presence of frequency multipath typically encountered in aeronautical telemetry. An adaptive decision feedback equalizer, suitable for use with SOQPSK in an iterative processing loop, is developed. It is shown that this equalizer is capable of achieving performance close to that of the MAP equalizer.

This paper is organized as follows: the SOQPSK modulation and the system model are described in Section II and Section III, respectively. The MAP turbo equalizer and the iterative decision feedback equalizer are presented in Section IV. In Section IV, the bit error rate performance of these equalizers for SOQPSK in the presence of multipath interference typical of that encountered in aeronautical telemetry is summarized and the conclusions are drawn in Section V.

SOQPSK-TG

Shaped offset QPSK (SOQPSK) is a ternary CPM modulation whose modulation index is $h = 1/2$. Using complex baseband notation, the SOQPSK waveform may be represented as

$$s(t) = \exp\{j\phi(t)\} \tag{1}$$

$$\phi(t) = \pi \sum_{n} \alpha_n g(t - nT_b) \tag{2}$$

where $\alpha_n \in \{-1, 0, +1\}$ is the n-th ternary symbol, T_b is the bit time, and $g(t)$ is a phase pulse that is the time integral of a frequency pulse $p(t)$ with area 1/2. The frequency pulse for SOQPSK-TG

is a *spectral* raised cosine pulse that is been windowed by a *temporal* raised-cosine. The phase and frequency pulses for SOQPSK-TG are given by [10]

$$g(t) = \int_{-\infty}^{t} p(x)dx \tag{3}$$

$$p(t) = A\frac{\cos\left(\frac{\pi\rho Bt}{2T_b}\right)}{1-4\left(\frac{\rho Bt}{2T_b}\right)^2} \times \frac{\sin\left(\frac{\pi Bt}{2T_b}\right)}{\frac{\pi Bt}{2T_b}} \times w_n(t) \tag{4}$$

where the window is given by (5) and the constant A is chosen to make the area of $p(t)$ 1/2. The waveform is completely specified by the parameters ρ, B, T_1, and T_2.

$$w_n(t) = \begin{cases} 1 & 0 \le \left|\frac{t}{2T_b}\right| \le T_1 \\ \frac{1}{2} + \frac{1}{2}\cos\left(\frac{\pi}{T_2}\left(\frac{t}{2T_b} - T_1\right)\right) & T_1 \le \left|\frac{t}{2T_b}\right| \le T_1 + T_2 \\ 0 & T_1 + T_2 < \left|\frac{t}{2T_b}\right| \end{cases} \tag{5}$$

For SOQPSK-TG the values are $\rho = 0.7$, $B = 1.25$,$T_1 = 1.5$, and $T_2 = 0.5$. The frequency pulse has support on the interval $-2 \le t/2T_b \le 2$ and thus spans 8 bit times. The mapping from binary input bits $c_n \in \{-1, 1\}$ to ternary symbols $\alpha_n \in \{-1, 0, 1\}$ is given by [11]

$$\alpha_n = (-1)^{n+1}\frac{c_{n-1}\left(c_n - c_{n-2}\right)}{2}. \tag{6}$$

The name "shaped offset QPSK" follows from the observation that each ternary symbol causes the carrier phase either advance by $\pm\pi/2$ radians or to remain at its current value. When viewed on an I-Q plot, the carrier phase appears to migrate from quadrant to quadrant along the unit circle. By contrast, the carrier phase of (unshaped) offset QPSK migrates from quadrant to quadrant instantaneously. Since the phase pulse "shapes" the phase trajectory of the carrier from what it would be for unshaped OQPSK, the waveform has an interpretation as a "shaped" OQPSK.

SYSTEM MODEL

The system is illustrated in Figure 1 where single lines are used to denote purely real or purely imaginary signals and double lines are used to represent complex-valued signals. The data source produces binary i.i.d. information bits $\{a_i\}$ which are turbo-encoded to produce coded bits b_n. The coded bits are interleaved to form the bit sequence c_n The interleaved coded bits form the input to

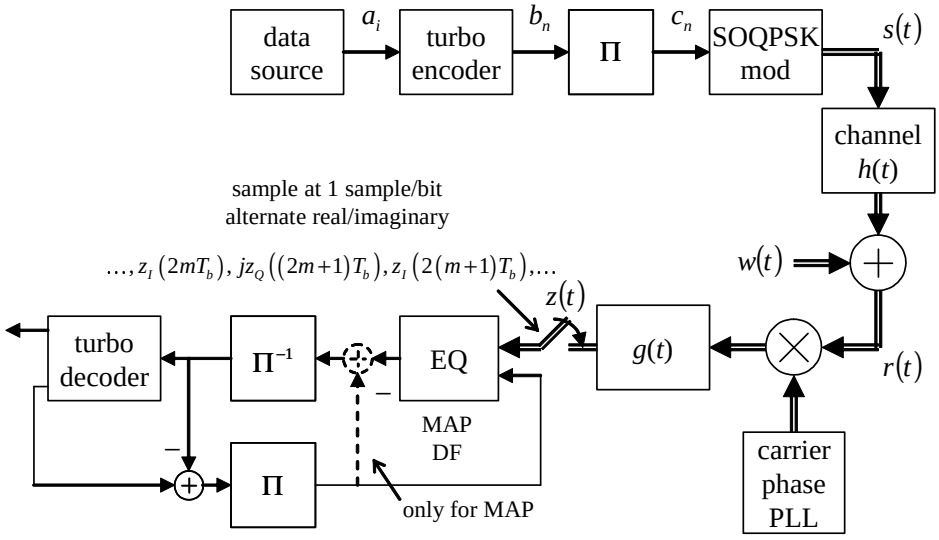

Figure 1: Block diagram of a generic iterative equalization system for SOQPSK.

an SOQPSK modulator.

The SOQPSK waveform (2) experiences multipath propagation that is modeled as an LTI system with impulse response $h(t)$. The received signal is

$$r(t) = s(t) * h(t) + w(t) \tag{7}$$

where $*$ is the convolution operation and $w(t)$ is the additive noise that is modeled as a complex-valued Gaussian random process with zero mean and power spectral density N_0 W/Hz.

After rotation by the carrier phase synchronizer, the received waveform $r(t)$ is filtered by a detection filter with impulse response $g(t)$, and sampled at T_b-spaced intervals to form the sequence $z(nT_b) = z_I(nT_b) + jz_Q(nT_b)$. The real part of $z(nT_b)$ for even n and the imaginary part of $z(nT_b)$ for odd n are retained and used for equalization, detection, decoding.[1] For this reason it will be convenient to represent the sampled matched filter outputs using even and odd indexes on the bit time as follows:

$$\ldots, z(2mT_b), z((2m+1)T_b), z(2(m+1)T_b), \ldots$$

The sequence

$$\ldots, z_I(2mT_b), jz_Q((2m+1)T_b), z_I((2(m+1))T_b), \ldots$$

forms the input to the iterative equalizer. The iterative equalizer attempts to mitigate the multipath interference using the sampled matched filter outputs and the extrinsic information supplied by the

[1]The discarded matched filter outputs — the imaginary part of $z(nT_b)$ for even n and the real part of $z(nT_b)$ for odd n — are used by the phase error detector in a carrier phase PLL and by the timing error detector in a symbol timing PLL.

turbo decoder. The soft outputs from the equalizer are deinterleaved and processed by the turbo decoder to produce the extrinsic information.

ITERATIVE EQUALIZATION FOR SOQPSK

Two iterative equalizers are explored here: the MAP equalizer and the adaptive decision feedback equalizer.

A. MAP Equalizer

The MAP equlizer is well known [12] and its form for (unshaped) OQPSK is fully described in [13]. The structure of the MAP equalizer combined with turbo encoder is illustrated in Figure 2. In this figure, the superscript *E* denotes the LLRs which are associated to the equalizer, whereas the superscript *D* reprents the turbo decoder's LLRs. The MAP equalizer computes the LLRs for the interleaved encoded bits $L^E(c_n)$ [14]. The extrinsic information for the interleaved coded bits, $L_e^E(c_n)$, is computed as shown and deinterleaved to form the extrinsic information for the coded bits $L_e^E(b_n)$. These values are used to compute the inputs for the turbo decoder $\tilde{b}_n$ using [5]

$$\tilde{b}_n = \left(\frac{\mathrm{E}\left\{ L_e^E\left(b_n\right)^2 \right\}}{2\left[\mathrm{E}\left\{ L_e^E\left(b_n\right) \operatorname{sgn}\left\{ L^E(b_n) \right\} \right\} \right]^2} - \frac{1}{2} \right) L_e^E\left(b_n\right). \tag{8}$$

where $L^E(b_n)$ is the LLR for b_n that is obtained by deinterleaving the MAP equalizer outputs $L^E(c_n)$. The turbo decoder generates the LLRs for the encoded bits, $L^D(b_n)$. The extrinsic information for b_n, $L_e^D(b_n)$, is computed as shown and interleaved to form the ***a priori*** estimates for the interleaved coded bits, $L_a^E(c_n)$, that is used as the input for the MAP equalizer for the next iteration.

The MAP turbo equalizer achieves the optimum performance, but the complexity grows exponentially with the ISI terms. Complexity can be reduced by using a suboptimum, reduced-complexity equalizer, such as an adaptive decision feedback equalizer, in place of the MAP equalizer as shown in the next subsection.

B. Iterative Decision Feedback Equalizer

The iterative equalizer using decision feedback for SOQPSK consists of two adaptive filters and a decision device arranged as shown in Figure 3. The first adaptive filter is an FIR feed-forward filter with L_{FF} (possibly complex) coefficients at time step n $w_{\mathrm{FF}}^{(n)}(k)$ for $k = -(L_{\mathrm{FF}}-1)/2, \ldots, (L_{\mathrm{FF}}-1)/2$. The output of the feed-forward filter, $z_0(n)$ is

$$z_0(n) = \sum_{l=-\frac{L_{\mathrm{FF}}-1}{2}}^{\frac{L_{\mathrm{FF}}-1}{2}} w_{\mathrm{FF}}^{(n)}(l) z(n-l) \tag{9}$$

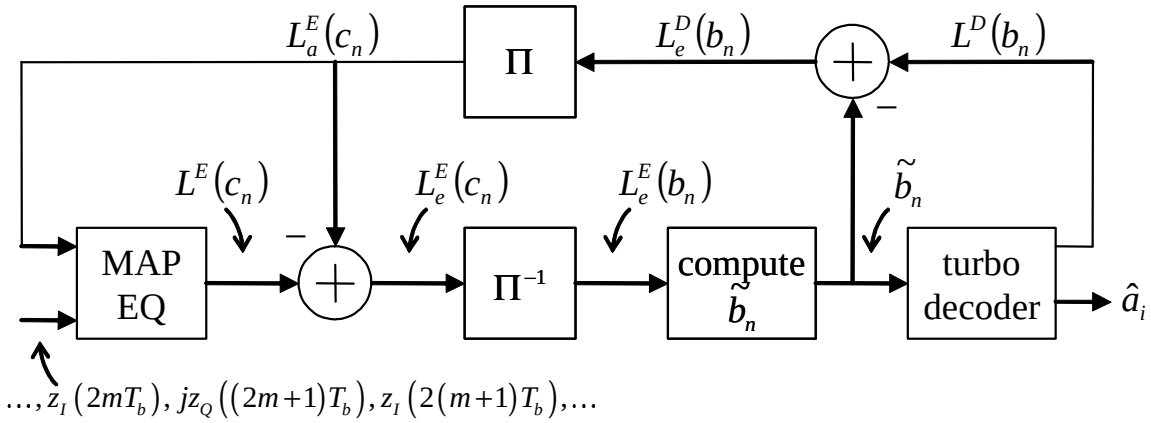

Figure 2: Block diagram of the MAP turbo equalizer.

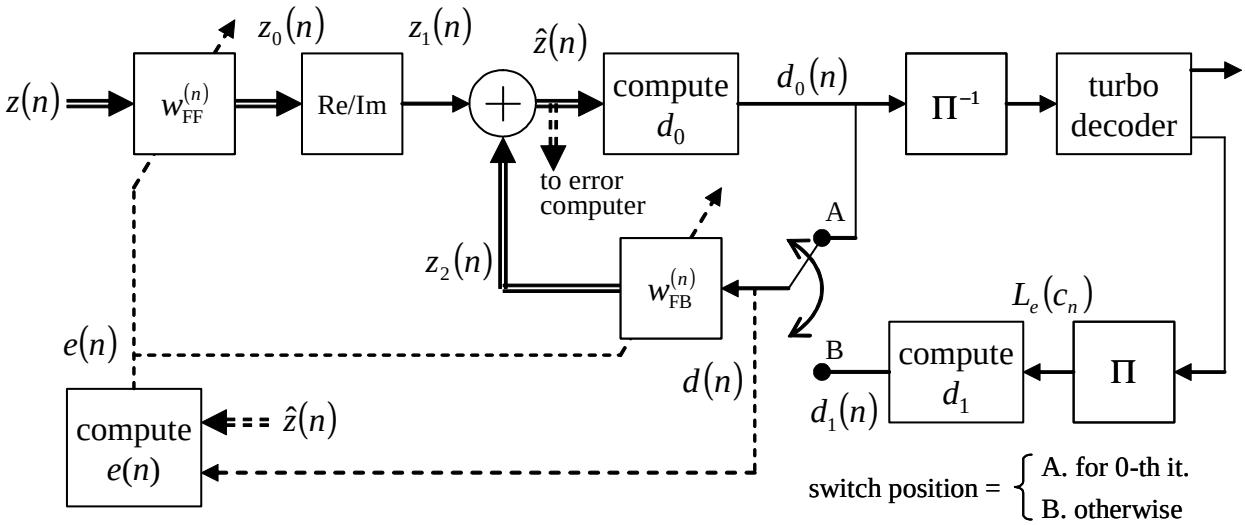

Figure 3: Block diagram of the proposed iterative decision feedback equalizer.

where $z(n)$ is a placeholder for the alternating sequence of real and imaginary components of the sampled matched filter outputs described in the previous section. Due to the offset nature of the modulation, only the real part of $z_0(n)$ need be considered for even n and the imaginary part of $z_0(n)$ for odd n. In recognition of this property, define $z_1(n)$ as

$$z_1(n) = \begin{cases} \text{Re}\left\{z_0(n)\right\} & n \text{ even} \\ j\text{Im}\left\{z_0(n)\right\} & n \text{ odd} \end{cases}. \tag{10}$$

This output is combined with $z_2(n)$, the output of the length L_{FB} feedback filter with coefficients at time step n $w_{\text{FB}}^{(n)}(l)$ for $l = 0, 1, \ldots, L_{\text{FB}} - 1$. The sum $\hat{z}(n) = z_1(n) + z_2(n)$ forms the soft output of the equalizer. The output of the feedback filter may be expressed as

$$z_2(n) = \sum_{l=0}^{L_{\text{FB}}-1} w_{\text{FB}}^{(n)}(l) d(n-l) \tag{11}$$

where $d(n)$ is the input to the feedback filter given by

$$d(n) = \begin{cases} d_0(n) & \text{0-th iteration} \\ d_1(n) & \text{otherwise} \end{cases} \tag{12}$$

Before the first iteration, the input to the decision feedback filter $d_0(n)$ is based on the decision. Due to the offset nature of the modulation, symbol decisions are based on $\hat{z}(n)$ using

$$d_0(n) = \begin{cases} \text{sgn}\left(\text{Re}\left\{\hat{z}(n)\right\}\right) & n \text{ even} \\ j\text{sgn}\left(\text{Im}\left\{\hat{z}(n)\right\}\right) & n \text{ odd} \end{cases}. \tag{13}$$

For subsequent iterations, $d_0(n)$ is

$$d_0(n) = \begin{cases} \text{Re}\left\{\hat{z}(n)\right\} & n \text{ even} \\ j\text{Im}\left\{\hat{z}(n)\right\} & n \text{ odd} \end{cases}. \tag{14}$$

From the first iteration on, the input to the decision feedback filter is $d_1(n)$ which is the mean symbol estimate of original symbol transmitted through the channel. The input to the turbo decoder is the sequence soft coded bit decisions denoted $\tilde{b_n}$. The soft coded bit decisions are obtained from the soft interleaved coded bit decisions $\tilde{c}_n$ by deinterleaving. The soft interleaved coded bit decisions are derived from $d_0(n)$ using

$$\tilde{c}_n = \begin{cases} d_0(n) & n \text{ even} \\ \text{Im}\left\{d_0(n)\right\} & n \text{ odd} \end{cases}. \tag{15}$$

The LLR output of the MAP decoder, $L^D(b_n)$, is used to compute the extrinsic information $L_e^D(b_n)$ as shown. The $L_e^D(b_n)$ are interleaved to form the $L_a^E(c_n)$, the ***a priori*** probability estimates of the c_n. These estimates are used to compute an equivalent mean symbol estimate using

$$d_1(n) = \begin{cases} \tanh\left(\dfrac{L_a^E(c_n)}{2}\right) & n \text{ even} \\ j\tanh\left(\dfrac{L_a^E(c_n)}{2}\right) & n \text{ odd} \end{cases}. \tag{16}$$

The update of both the feedforward and feedback filter coefficients is realized using the adaptive LMS algorithm [15]:

$$\begin{bmatrix} w_{\text{FF}}^{(n+1)}(-\frac{L_{\text{FF}}-1}{2}) \\ \vdots \\ w_{\text{FF}}^{(n+1)}(0) \\ \vdots \\ w_{\text{FF}}^{(n+1)}(\frac{L_{\text{FF}}-1}{2}) \end{bmatrix} = \begin{bmatrix} w_{\text{FF}}^{(n)}(-\frac{L_{\text{FF}}-1}{2}) \\ \vdots \\ w_{\text{FF}}^{(n)}(0) \\ \vdots \\ w_{\text{FF}}^{(n)}(\frac{L_{\text{FF}}-1}{2}) \end{bmatrix} + \mu e(n) \begin{bmatrix} z^*(n+\frac{L_{\text{FF}}-1}{2}) \\ \vdots \\ z^*(n) \\ \vdots \\ z^*(n-\frac{L_{\text{FF}}-1}{2}) \end{bmatrix}$$
$$\begin{bmatrix} w_{\text{FB}}^{(n+1)}(0) \\ w_{\text{FB}}^{(n+1)}(1) \\ \vdots \\ w_{\text{FB}}^{(n+1)}(L_{\text{FB}}-1) \end{bmatrix} = \begin{bmatrix} w_{\text{FB}}^{(n)}(0) \\ w_{\text{FB}}^{(n)}(1) \\ \vdots \\ w_{\text{FB}}^{(n)}(L_{\text{FB}}-1) \end{bmatrix} + \mu e(n) \begin{bmatrix} d^*(n) \\ d^*(n-1) \\ \vdots \\ d^*(n-L+1) \end{bmatrix} \tag{17}$$

where μ is the adjustable step size that controls the rate of convergence and coefficients error variance and $e(n)$ is the error based on the difference between the soft equalizer output $\hat{z}(n)$ and the decision $d(n)$:

$$e(n) = \begin{cases} d(n) - \text{Re}\left\{\hat{z}(n)\right\} & n \text{ even} \\ d(n) - j\text{Im}\left\{\hat{z}(n)\right\} & n \text{ odd} \end{cases}. \tag{18}$$

PERFORMANCE AND RESULTS

The performance of SOQPSK-TG using the MAP equalizer and the iterative decision feedback equalizer were simulated in the presence of multipath interference typical of that encountered in aeronautical telemetry [1]. The multipath interference can be modeled as an linear system with impulse response

$$h(t) = \delta(t) + \Gamma_1\delta(t-\tau_1) + \Gamma_2\delta(t-\tau_2). \tag{19}$$

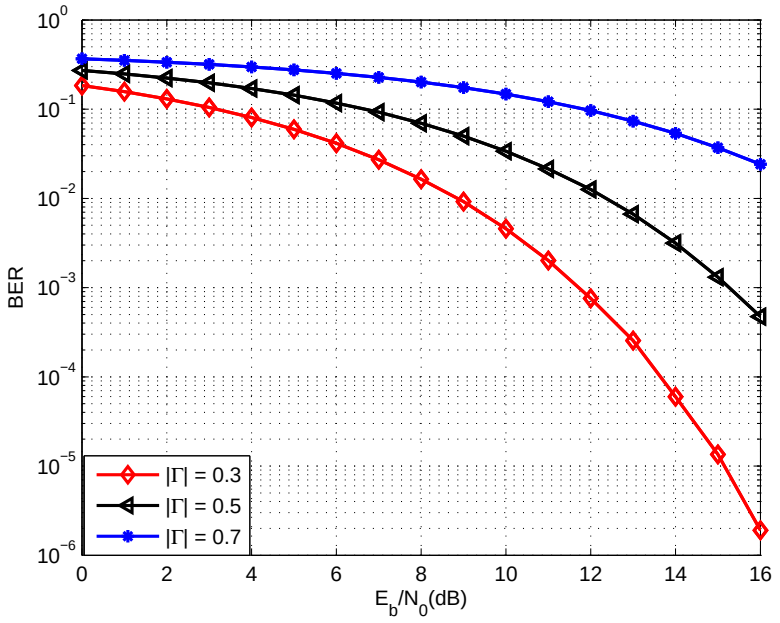

Figure 4: Performance of uncoded SOQPSK-TG over the channel 20 without equalization.

The first multipath component with complex amplitude Γ_1 and delay τ_1 is a result of a strong "ground bounce" off the dry lake beds typical of test ranges in the Western USA. These parameters are a function of the system geometry (i.e. the relative locations of the airborne transmitter and the receiver ground station). $|\Gamma_1|$ can be as large as 0.7 or 0.8 and the delay is typically in the $40-80$ ns range. At 20 M bits/sec, this delay is on the order of one bit time. The second multipath component with amplitude Γ_2 and delay τ_2 is due to reflections from irregular terrain. As a consequence, the multipath component is much more random with $|\Gamma_2|$ on the order of 0.01 and τ_2 on the order of a few hundred ns. In the simulations that follow, the channel impulse response is

$$h(t) = \delta(t) + |\Gamma_1|e^{j\pi}\delta(t - T_b). \tag{20}$$

The phase of Γ_1 was set to π to position the spectral null due to the multipath in the center of the spectrum to generate the worst-case scenario for this channel. $|\Gamma_1|$ was set to $0.3, 0.5$ and 0.7 to monitor equalizer performance as a function of the relative strength of the multipath interference. In the simulation, the turbo code was a rate-$1/3$ code with two identical recursive systematic encoders with generator polynomials, expressed in octal, $(15, 17)$. The encoders were separated by a S-random interleaver [16] where the interleaver block size was $K_c = 2048$ and $S = 0.5\sqrt{0.5K_c} = 16$. The same interleaver was used between the turbo encoder and the SOQPSK modulator. A length-500 bit training sequence was used to train the adaptive filters in the decision feedback equalizer. The LMS step size was $\mu = 10^{-6}$ for both training and tracking. The filter lengths were $L_{\text{FF}} = 19$ and $L_{\text{FB}} = 9$.

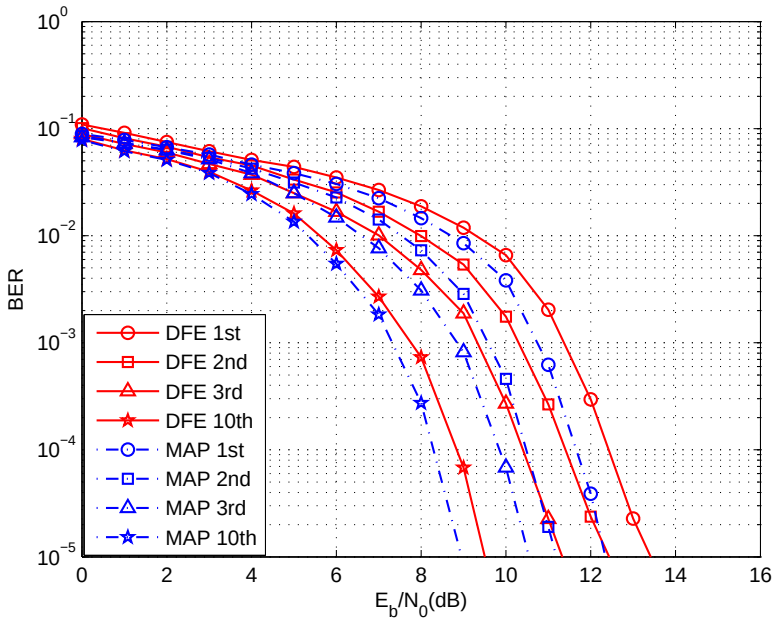

Figure 5: Performance of SOQPSK-TG with MAP Equalizer and decision feedback equalizer over the channel 20 with $|\Gamma_1| = 0.3$.

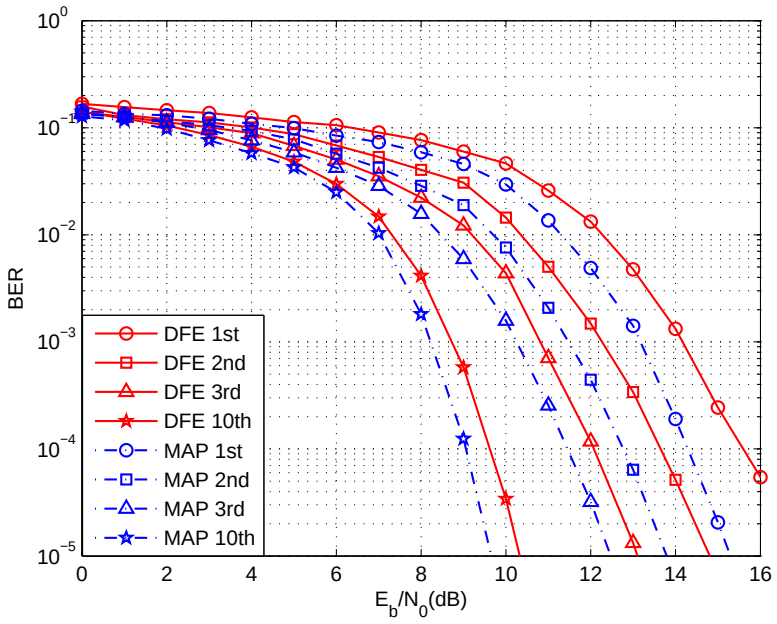

Figure 6: Performance of SOQPSK-TG with MAP equalizer and decision feedback equalizer over the channel 20 with $|\Gamma_1| = 0.5$.

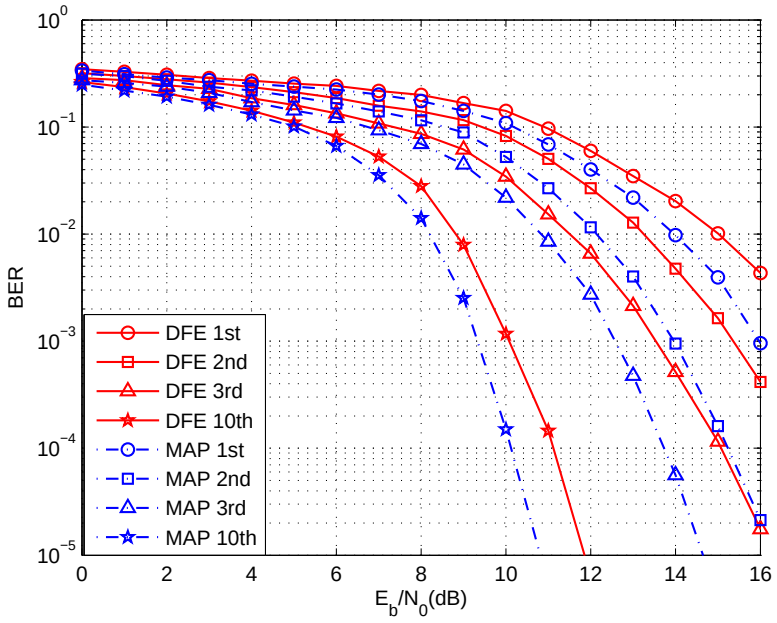

Figure 7: Performance of SOGPSK-TG with MAP equalizer and decision feedback equalizer over the channel 20 with $|\Gamma_1| = 0.7$.

Figure 4 shows the bit error rate performance of unequalized SOQPSK-TG which is provided for reference. The bit error rate performance of the MAP equalizer and the adaptive decision feedback equalizer for $|\Gamma_1| = 0.3, 0.5, 0.7$ are plotted in Figures 5, 6, and 7, respectively. In each plot, the bit error rate performance after the first, second, third, and tenth iterations is also shown. The simulation results show that as the number of iterations increases, the performance of the two considered equalizers improve impressively. The simulation results for decision feedback equalizer after 10 iterations at a bit error rate of 10^{-5} are summarized in Table 1.

CONCLUSIONS

An iterative decision feedback equalizer suitable for use with SOQPSK-TG was presented and compared with MAP turbo equalizer. Simulation results demonstrate that in the presence of frequency selective multipath typically encountered in aeronautical telemetry, the proposed adaptive turbo equalizer offers good complexity/performance trade-offs and exhibits impressive performance close to the MAP turbo equalizer for SOQPSK-TG.

Table 1: Performance summary of the decision feedback equalizer

$\|\Gamma\|$	gain relative to uncoded/unequalized system (dB)	loss relative to MAP equalizer (dB)
0.3	5.6	0.5
0.5	8.2	0.7
0.7	12.1	1.1

References

[1] M. Rice, A. Davis, and C. Bettwieser, "A wideband channel model for aeronautical telemetry," *IEEE Transactions on Aerospace and Electronic Systems*, vol. 40, no. 1, pp. 57–69, January 2004.

[2] M. Rice and Q. Lei, "SHF multipath channel modeling results," in *Proceedings of the International Telemetering Conference*, Las Vegas, NV, October 2005, pp. 101–110.

[3] J. Proakis, *Digital Communications*. McGraw-Hill, 2001.

[4] C. Douillard *et al.*, "Iterative correction of intersymbol interference: Turbo equalization," *European Transactions on Telecommunications*, vol. 6, pp. 507–511, September/October 1995.

[5] D. Raphaeli and Y. Zarai, "Combined turbo equalization and turbo decoding," in *IEEE GLOBECOM*, 1997, pp. 639–643.

[6] M. Tüchler, R. Koetter, and A. Singer, "Turbo equalization: principles and new results," *IEEE Transactions on Communications*, vol. 50, pp. 754–767, May 2002.

[7] C. Laot, A. Glavieux, and J. Labat, "Turbo equalization: adaptive equalization and channel decoding jointly optimized," *IEEE Journal on Selected Areas in Communications*, vol. 19, no. 9, September 2001.

[8] D. Raphaeli and A. Saguy, "Linear equalization for turbo equalization a new optimization criterion for determining the equalizer taps," in *Proceedings of the 2nd Symposium on Turbo Codes and Related Topics*, Brest, France, September 2000, pp. 371–374.

[9] *IRIG Standard 106-00: Telemetry Standards*, Range Commanders Council Telemetry Group, Range Commanders Council, White Sands Missile Range, New Mexico, 2000, (Available on-line at http://jcs.mil/RCC/manuals/106-00).

[10] T. Hill, “An enhanced, constant envelope, interoperable shaped offset QPSK (SOQPSK) waveform for impoved spectral efficiency,” in *Proceedings of the International Telemetering Conference*, San Diego, CA, October 2000, pp. 127–136.

[11] L. Li and M. K. Simon, “Performance of coded OQPSK and MIL-STD SOQPSK with iterative decoding,” *IEEE Transactions on Communications*, vol. 52, pp. 1890–1900, November 2004.

[12] R. Koetter, A. Singer, and M. Tüchler, “Turbo equalization,” *IEEE Signal Processing Magazine*, vol. 21, pp. 67–80.

[13] Q. Lei and M. Rice, “Iterative equalization for offset QPSK in frequency selective multipath,” in preparation for submitting to IEEE Communications Letters.

[14] M. Tüchler, A. Singer, and R. Koetter, “Minumum mean square error equalization using a priori information,” *IEEE Transactions on Signal Processing*, vol. 50, no. 3, March 2002.

[15] S. Haykin, *Adaptive Filter Theory*. Prentice-Hall, 2001.

[16] D. Divsalar and F. Pollara, “Multiple turbo codes for deep-space communications,” in *Telecommunications and Data Acquisition Progress Report*, May 1995, pp. 42–121.